THE JOURNAL OF PHYSICAL CHEMISTRY Letters

Letter

pubs.acs.org/JPCL

Stability of Positively Charged Solutes in Water: A Transition from Hydrophobic to Hydrophilic

Tod A Pascal,[†,‡] Shiang-Tai Lin,[§] William Goddard, III,*[,†,‡] and Yousung Jung*[,†]

[†]Graduate School of EEWS (WCU), Korea Advanced Institute of Science and Technology, Daejeon, Korea

[‡]Materials and Simulation Process Center, California Institute of Technology, Pasadena, California 91125, United States

[§]Department of Chemical Engineering, National Taiwan University, Taipei 10617, Taiwan

Supporting Information

ABSTRACT: To improve the description of solvation thermodynamics of biomolecules, we report here the dependence of solvation on the curvature and surface charge of positively charged solutes in water based on extensive molecular dynamics simulations analyzed using the two-phase thermodynamic method. At a surface charge of +0.4e, the compensating forces of favorable electrostatic stabilization and entropic destabilization cancel almost exactly, representing a molecular crossover point from hydrophobic to hydrophilic behavior, independent of curvature. These results suggest that one should include charge-dependent entropic corrections to continuum models aimed at predicting the solvation free energies of large biomolecules.

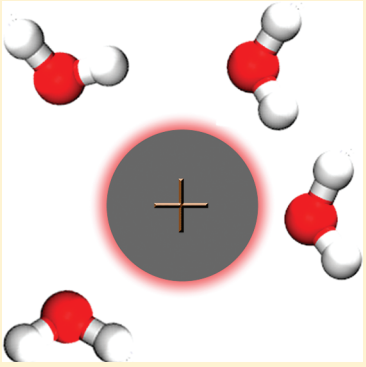

SECTION: Statistical Mechanics, Thermodynamics, Medium Effects

The solute−water interactions that determine the solubility of biomolecules such as proteins and DNA in water depend on size, geometry, and surface character. Due to this complexity, simplified models have been employed to obtain a qualitative understanding of the forces that determine stability. For example, from calculations of the change in the free energy of water due to the presence of spherical, nonpolar solutes of increasing size, several studies[1−3] have proposed the existence of an entropic driving force for assembly of large proteins in water.[5,6] The solutes in these studies are hydrophobic, in sharp contrast to solvation of real ions, which are strongly hydrophilic and characterized by large solvation free energies. The extreme case is that of the proton (H^+), where both experiments[7,8] and theory[9] estimate a solvation energy of −1050 kJ/mol.

Theoretical studies on the solvation of ions in water revealed a quadratic dependence on charge,[10] although the polarizability of the ions as well as the asymmetry of the water molecule and the tendency for water to hydrogen bond to anions lead to a measurable difference in the solvation thermodynamics of similarly sized cations and anions.[11,12] Other studies have shown that nanoscale solutes can be hydrophobic while having a surface charge distribution.[13−15] Experimentally, a femtosecond mid-infrared spectroscopy study suggested that hydrophobic groups are surrounded by effectively immobilized water molecules in the first solvation shell,[16] a claim that has been disputed.[17] More recently, picosecond and femtosecond X-ray absorption spectroscopy was used to probe the changes of the solvent shell structure upon electron abstraction of aqueous iodide using an ultrashort laser pulse,[18] demonstrating that large ions may display hydrophobic behavior in solution.

These studies and others all indicate a charge-dependent, molecular crossover point from hydrophobic to hydrophilic character, although this has not been clearly demonstrated. Here, we quantify the entropic penalty of ordered water structure due to electrostatic attractions between charged species and water at the interface, which affects the interfacial properties of water so important for such basic phenomena as dissolution. Thus, we address these issues by explicitly calculating the entropy ($T\Delta S^0$) and free energy (ΔA^0) of water in the presence of a variable sized solute of charge states ranging from 0 to +1e.

Our results are based on extensive molecular dynamics simulations using the LAMMPS[19] simulation engine in the isobaric (1 atm), isothermal (298 K), or *NPT* ensemble. Spherical cavities with hard-sphere radii of $0 \leq r_{HC} \leq 15$ Å were created inside of pre-equilibrated cubic water boxes (216−3305 water molecules) described using the extended simple point charge (SPC/E) water potential.[20] The SPC/E water model has been extensively used in solvation studies[4,11,13,21] and is used here for convenience and computational efficiency. We note that while the solvation thermodynamics is somewhat sensitive to the choice of water model,[11,21−23] the solvation trends should be less so, if only due to cancellation of errors.

Received: December 7, 2011
Accepted: January 6, 2012

We initiate the simulations by removing any water molecules in the interior and within 2 Å of the virtual solute surface while ensuring a 10 Å water buffer in each direction (Table S1 of Supporting Information). The oxygen atoms interact with the closest contact point on the surface of the solute (Figure 1)

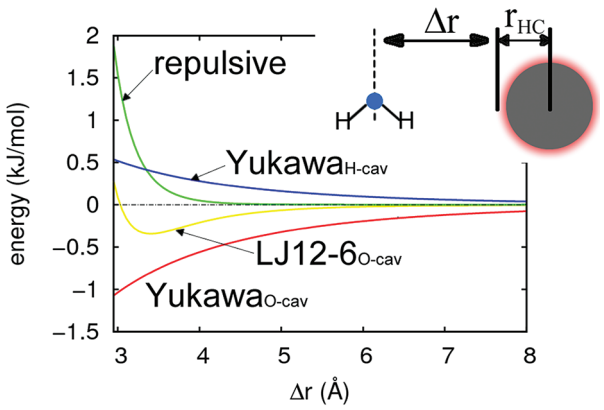

Figure 1. Interaction potentials of the oxygen on water with repulsive $E_{rep} = 1.368[(3.03/\Delta r)^{12}]$ (green), attractive $E_{LJ12-6} = 1.368[(3.03/\Delta r)^{12} - (3.03/\Delta r)^{6}]$ (yellow) solutes used in this study. The hydrogen (blue, $q_i = +0.4238$) and oxygen (red, $q_i = -0.8476$) of the water molecules also interact with the solutes electrostatically through Yukawa potentials $E_{Yukawa} = 98.7(q_i q_j/\Delta r)e^{-0.33\Delta r}$ where q_j is the surface charge of the solute. The Yukawa potentials are scaled by a factor of 10 for presentation purposes. All potentials are tapered smoothly to zero from 7−8 Å using a 7th order taper function (not shown).

through a Lennard-Jones 12−6 (LJ12−6) potential, assuming the parameters of helium[24] and geometric combination rules with the SPC/E parameters, $\varepsilon_{ij} = (\varepsilon_i\varepsilon_j)^{1/2}$ and $\sigma_{ij} = (\sigma_i\sigma_j)^{1/2}$, which result in $\varepsilon = 0.342$ kJ/mol and $\sigma = 3.03$ Å. By requiring that the water molecule interact with the solute surface, we guarantee that the water molecules feel a uniform field, irrespective of solute curvature, thus allowing unambiguous probing of the curvature effect.

We approximate the electrostatic interactions using a Yukawa (screened coulomb) potential

$$E_{elec} = A\frac{q_i q_j}{r}e^{-\kappa r} \quad (1)$$

where q_i is the charge of oxygen (-0.8476 e$^-$) or hydrogen ($+0.4238$ e$^-$), q_j is the surface charge of the solute, $A = 98.7$ kJ/mol is an energy conversion parameter, and the Debye screening length $1/\kappa = 3$ Å represents a 1.0 M ion concentration. Because we are simulating an infinitely periodic system, the unit cell necessarily needs to be neutral. Thus, our choice of a Yukawa potential circumvents the need to place a compensating charge in the unit cell or application of neutralizing background corrections to the energies. While this choice may appear limiting, we show later that our description of the electrostatics give results in good agreement with explicit charge calculations. We further require that the energy and forces of our interaction potentials converge smoothly to zero at 8 Å by means of a seventh-order taper function.

We performed 5 ns of *NPT* equilibration dynamics followed by an additional 5 ns of production dynamics for each system. The temperature coupling constant was 0.1 ps, while the pressure piston constant was 2.0 ps. The long-range electrostatics interactions were evaluated by the PPPM method, with a Ewald tolerance parameter of 10e^{-4}. Absolute entropies and quantum corrections to the internal energy were calculated from additional 20 ps MD trajectories using the two-phase thermodynamic (2PT) method[25] every 100 ps. Convergence in the thermodynamics was obtained after 0.5 ns.

In the 2PT method, the density of states of the system was obtained from a Fourier transform of the integrated velocity autocorrelation function. The diffusive component of the power spectrum was extracted, and the thermodynamics were determined from hard-sphere theory, while the thermodynamics of the remaining component were determined from Debye theory of a vibrating crystal. The 2PT method has been validated to reproduce the free energy of liquid water along the water−vapor coexistence curve[26] and for bulk water from classical[26] and ab initio MD trajectories,[27] and recently, it was used to determine the thermodynamics of water confined in carbon nanotubes,[28] hydrogels,[29] and the stability of hydrocarbons.[30] We exploit the efficiency of the 2PT method when calculating the system thermodynamics at 100 ps intervals over the final 5 ns of dynamics. The reported statistics are the average of 50 data points, representing a mere 10% increase in computational time, while the quoted deviations are the measured variance.

Of course, the various approximations made in our model will have to be validated on proven systems. We do this by calculating the solvation free energy of monovalent cations ($R_{HC} = 0$ in all cases, i.e., an imaginary point charge without size) by combining recently reported LJ12−6 parameters,[21] our solute model, and the Yukawa potential (without any adjustments). As detailed in Table S2 (Supporting Information), the solvation free energies of Li^+ ($\Delta G^0 = -442.22$), Na^+ ($\Delta G^0 = -399.60$), and K^+ ($\Delta G^0 = -306.18$) show a 98% correlation with experiments[8,31] and overall good agreement with previous computational results.[32,33] Coulombic potentials are long-ranged; therefore, our results using short-range potentials may appear surprising. Previous simulations results have indeed shown that using similar interaction potentials accurately captures the solvation thermodynamics of real ions in water.[34] Thus, we reason that the Coulombic field produces highly localized perturbation of the water structure around the ion that does not disrupt the longer-range hydrogen-bonding network. This is consistent with femtosecond pump−probe[35] and vibrational O−H spectroscopic[36] studies, which demonstrated that the respective rotational and vibrational dynamics of water around small ions converge to the bulk beyond the first solvation shell.

Figure 2 shows the energies of solute solvation, referenced to a bulk water box. As expected, the hydrophilicity of the solute increases with increasing surface charge; for He^0, it ranges from +22.6 kJ/mol at $R_{HC} = 0$ to +1565.9 kJ/mol at $R_{HC} = 15$ Å, while for He^+, it ranges from −139.5 kJ/mol for $R_{HC} = 0$ to −3239.8 kJ/mol at $R_{HC} = 15$ Å. In other words, the surface tension γ_∞ (i.e., the change in free energy per unit surface area)

$$\gamma_\infty = \frac{\Delta A^0}{4\pi R^2} \quad (2)$$

at the macroscopic limit decreases with increasing surface charge. It is +61.3 dyn/cm for neutral solutes with LJ12−6 surface potentials to +50.5 dyn/cm for 0.3 e and −130.1 dyn/cm for 1.0 e solutes. As a figure of merit, the calculated surface tension, extrapolated to the macroscopic limit, of a neutral repulsive solute (meant to mimic the air−water interface) is

dx.doi.org/10.1021/jz201612y | J. Phys. Chem. Lett. 2012, 3, 294−298

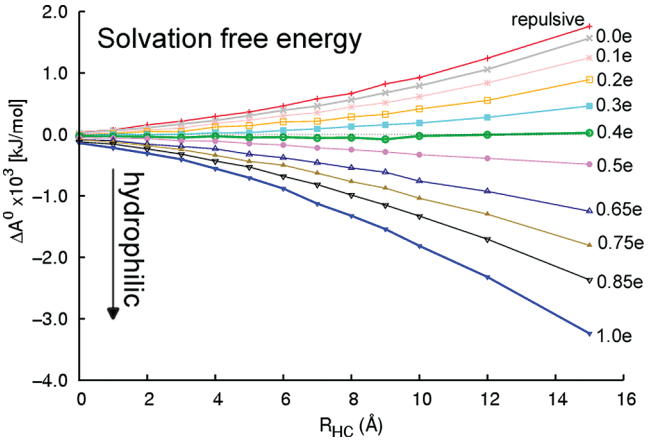

Figure 2. Free-energy cost solvation from explicit MD simulations and the 2PT method for creation of solutes of various sizes R_{HC} for various surface charge states from 0 to +1 e. The hydrophilicity of the solute increases with increasing surface charge, crossing over from hydrophobic to hydrophilic behavior at +0.4 e. A purely repulsive solute (red) is referenced.

67.0 dyn/cm, which is in reasonable agreement with the range of 73.6−71.8 dyn/cm from previous studies using the SPC/E water model[37] and with 72 dyn/cm from experiment (Figure 3).

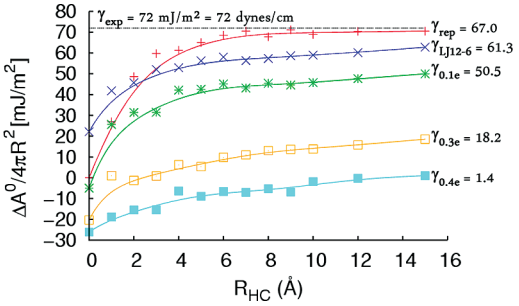

Figure 3. Change in the surface tension ($\Delta A^0/dA$) of the SPC/E water box with solutes of total radius R ($R = R_{HC} + R_s$, where R_s = 1.8 Å is the radii of a water molecule). The solid lines are best-fit Bezier functions of the data points. γ_{exp} is the experimental surface tension of water, γ_{rep} is the surface tension using a purely repulsive surface potential (red), γ_{LJ12-6} is the apolar LJ12−6 surface potential (blue), and $\gamma_{0.1e}$ (green), $\gamma_{0.3e}$ (brown), and $\gamma_{0.4e}$ (cyan) are for LJ12−6 surface potentials with 0.1, 0.3, and 0.4e excess Coulombic charges, respectively.

The solvation free energy of solutes with +1 e surface charge decreases monotonically with radii. This result is in contrast with the relationship between solvation free energies and ionic radii of the alkali ions, Li^+ (0.9 Å) < Na^+ (1.16 Å) < K^+ (1.52 Å) < Rb^+ (1.66 Å). This apparent discrepancy arises from the difference in the ion-dependent versus size-independent short-range London dispersive force and Pauli repulsion. The Pauli repulsion is a measure of the "hardness" or atomic polarizability and varies with radii; a measure of this variance can be obtained by comparing the ε and σ parameters in Table S1 (Supporting Information). Our approach, on the other hand, of using the same He parameters for all solutes was chosen to isolate the curvature and charge effects on the solvation, which allows a more systematic investigation of solvation thermodynamics. In other words, the short-range forces conspire to determine the solvation free energy of real ions in water in ways that cannot be captured by ionic radii alone as in our model solutes.

Interestingly, we find that a surface charge of 0.4 e corresponds to the molecular crossover point from hydrophobic to hydrophilic behavior. The thermodynamic cost of solute creation is near zero for small solutes (−26.6 ± 10.9 kJ/mol at R_{HC} = 0), intermediate (−44.9 ± 15.7 kJ/mol at R_{HC} = 6 Å) for intermediate-sized solutes, and large (25.0 ± 30.2 kJ/mol at R_{HC} = 15 Å) for large solutes. Indeed, for q = +0.4 e, the calculated solvation free energy is found to be close to zero over the entire range of solute sizes (Figure 2), indicating that at this surface charge, the surface tension is nearly zero and water molecules view the solute as if it were another water molecule. It is interesting to note that the hydrophobic/hydrophilic crossover point of q = +0.4 e is practically equal to the charge of the water H atom in the SPC/E model (+0.417 e), thus underscoring the delicate balance between dispersive and electrostatic forces in liquid water.

Further insights into the nature of the thermodynamics at various charge states can be obtained by separately considering the enthalpic and entropic components of the free energy (see Figure 4)

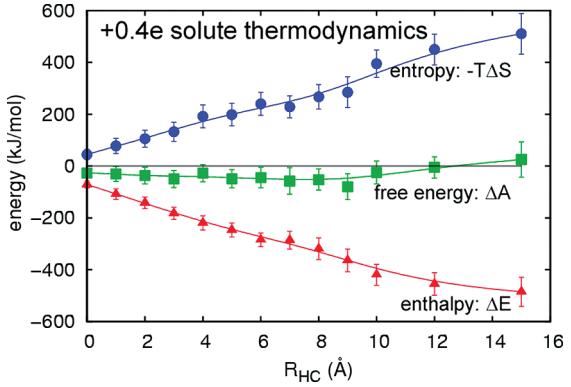

Figure 4. Components of the free energy (green squares) of the +0.4 e solute as a function of solute radius. The total entropy ($-T\Delta S$, blue circles) and enthalpy (red triangles) cancel almost exactly for all solute sizes, resulting in a net zero solvation free energy. The data points are smooth with a Bezier function (lines) for presentation purposes, and uncertainties are indicated by vertical bars.

$$\Delta A^0 = \Delta E^0 - T\Delta S^0 \quad (3)$$

where the free water box[26] is taken as the reference. For typical nonpolar solutes,[4] the solvation entropy is unfavorable for $R_{HC} \leq 6$ Å and then crosses over, becoming favorable for larger solutes (see the inset of Figure 5). This crossover is related to a transition from a molecular-sized surface to a bulk interface where dangling OH bonds appearing at the interface lead to enhanced rotational and translational entropy and hence increased entropy. In contrast, solutes with +0.4 e surface charge have unfavorable entropy and are destabilized for all sizes without such a transition. In fact, all positively charged solutes have unfavorable entropy for all sizes (Figure 5) due to the increased ordering of the water structure near the surface.

On the other hand, the additional electrostatic interactions stabilize the solutes, overcoming both the entropic loss due to a stronger and more rigid binding of water molecules and the energy loss due to broken hydrogen bonds at the interface for

dx.doi.org/10.1021/jz201612y | J. Phys. Chem. Lett. 2012, 3, 294−298

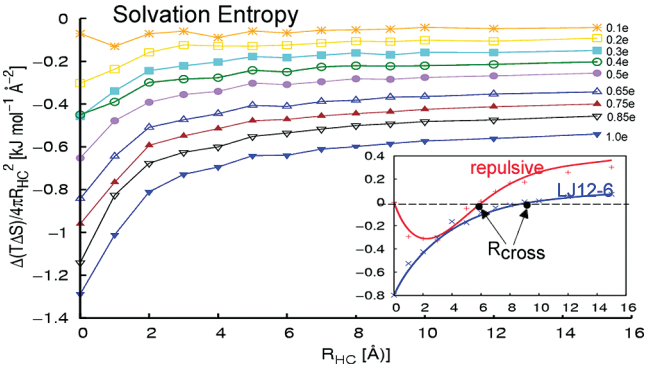

Figure 5. Relative entropy per unit surface area of charged solutes, relative to the nonpolar LJ12−6 solutes ($\Delta[T\Delta S]/dA$. The color scheme is the same as that in Figure 1. (Inset) Comparison of repulsive (red circles) and LJ12−6 (blue squares) solutes. The crossover radius, R_{cross}, where the entropy crosses zero at 298 K is calculated to be 6.0 Å for the repulsive solute, in general agreement with results from scaled particle theory.[4] The additional dispersive interactions of the LJ12−6 solutes shifts R_{cross} to 9.8 Å.

large solutes. More generally, the additional electrostatic forces in positively charged solutes have the effect of enthalpic stabilization and entropic destabilization. The interplay of these two competing forces, coupled with the thermodynamics of hydrophobic aggregation,[38] determines the system thermodynamics. Thus, for surface charges between 0 and +0.4 e, solutes are hydrophobic and prefer to aggregate in solution due to an unfavorable solvation free energy, while for larger surface charges, the tendency would be spontaneous dispersion throughout the liquid.

Of course the effect of negative surface potentials must be similarly quantified to obtain a complete description of the solvation thermodynamics. Our simplified description of the electrostatics underestimates the solvation free energy of negatively charges solutes by as much as 70%. This is because water molecules should form additional hydrogen-bonding interactions with such solutes,[12] an effect that is not be captured effectively by our model. This discrepancy cannot be remedied by simply applying a hydrogen bond correction to our solvation free energies as the hydrogen bonding alters the dynamics of water around the solute.

In summary, we presented a transition of the charged solutes from its character of being hydrophobic to being hydrophilic at a partial charge of 0.4 e. At this partial charge, the surface tension becomes zero due to a balance between unfavorable entropy (ordered and strongly bound water molecules) and favorable enthalpy (electrostatic stabilization). These results suggest charge-dependent entropic corrections to continuum models aimed at predicting the solvation free energies of large biomolecules, which conventionally have not considered the charge dependence in calculating the energy of cavity formation. Indeed, due to the asymmetry of the water molecule and the very different character of the first solvation shell,[39] it has been suggested that simplified models of implicit solvation will have to be augmented in order to quantitatively describe the solvation phenomenon.[40] We believe that the results presented here can be one route to obtaining such corrections, possibly by surface area correction to the entropy, based on the charge of the atoms at the surface.

■ ASSOCIATED CONTENT

Supporting Information

Tables of simulation setup and energies. This material is available free of charge via the Internet at http://pubs.acs.org.

■ AUTHOR INFORMATION

Corresponding Author

*E-mail: wag@wag.caltech.edu (W.G.); ysjn@kaist.ac.kr (Y.J.).

■ ACKNOWLEDGMENTS

This work was supported by the National Research Foundation of Korea (WCU R31-2008-000-10055-0, 2010-0029034) with partial support by grant NSC 100-2221-E-002-175 from the National Science Council of Taiwan. The authors acknowledge the generous allocation of supercomputing time from the KISTI supercomputing center at KAIST.

■ REFERENCES

(1) Swope, W. C.; Andersen, H. C. A Molecular Dynamics Method for Calculating the Solubility of Gases in Liquids and the Hydrophobic Hydration of Inert-Gas Atoms in Aqueous Solution. *J. Phys. Chem.* **1984**, *88*, 6548−6556.

(2) Huang, D. M.; Chandler, D. The Hydrophobic Effect and the Influence of Solute−Solvent Attractions. *J. Phys. Chem. B* **2002**, *106*, 2047−2053.

(3) Hummer, G.; Garde, S.; Garcia, A. E.; Paulaitis, M. E.; Pratt, L. R. Hydrophobic Effects on a Molecular Scale. *J. Phys. Chem. B* **1998**, *102*, 10469−10482.

(4) Ashbaugh, H. S. Entropy Crossover from Molecular to Macroscopic Cavity Hydration. *Chem. Phys. Lett.* **2009**, *477*, 109−111.

(5) Chandler, D. Interfaces and the Driving Force of Hydrophobic Assembly. *Nature* **2005**, *437*, 640−647.

(6) Chandler, D.; Huang, D. M. Temperature and Length Scale Dependence of Hydrophobic Effects and Their Possible Implications for Protein Folding. *Proc. Natl. Acad. Sci. U.S.A.* **2000**, *97*, 8324−8327.

(7) Coe, J. V.; Tissandier, M. D.; Cowen, K. A.; Feng, W. Y.; Gundlach, E.; Cohen, M. H.; Earhart, A. D.; Tuttle, T. R. The Proton's Absolute Aqueous Enthalpy and Gibbs Free Energy of Solvation from Cluster−Ion Solvation Data. *J. Phys. Chem. A* **1998**, *102*, 7787−7794.

(8) Marcus, Y. Thermodynamics of Solvation of Ions 0.5. Gibbs Free-Energy of Hydration at 298.15-K. *J. Chem. Soc., Faraday Trans.* **1991**, *87*, 2995−2999.

(9) Tawa, G. J.; Topol, I. A.; Burt, S. K.; Caldwell, R. A.; Rashin, A. A. Calculation of the Aqueous Solvation Free Energy of the Proton. *J. Chem. Phys.* **1998**, *109*, 4852−4863.

(10) LyndenBell, R. M.; Rasaiah, J. C. From Hydrophobic to Hydrophilic Behaviour: A Simulation Study of Solvation Entropy and Free Energy of Simple Solutes. *J. Chem. Phys.* **1997**, *107*, 1981−1991.

(11) Rajamani, S.; Ghosh, T.; Garde, S. Size Dependent Ion Hydration, Its Asymmetry, and Convergence to Macroscopic Behavior. *J. Chem. Phys.* **2004**, *120*, 4457−4466.

(12) Bakker, H. J.; Tielrooij, K. J.; Garcia-Araez, N.; Bonn, M. Cooperativity in Ion Hydration. *Science* **2010**, *328*, 1006−1009.

(13) Hua, L.; Zangi, R.; Berne, B. J. Hydrophobic Interactions and Dewetting between Plates with Hydrophobic and Hydrophilic Domains. *J. Phys. Chem. C* **2009**, *113*, 5244−5253.

(14) Giovambattista, N.; Debenedetti, P. G.; Rossky, P. J. Effect of Surface Polarity on Water Contact Angle and Interfacial Hydration Structure. *J. Phys. Chem. B* **2007**, *111*, 9581−9587.

(15) Wang, C.; Lu, H.; Wang, Z.; Xiu, P.; Zhou, B.; Zuo, G.; Wan, R.; Hu, J.; Fang, H. Stable Liquid Water Droplet on a Water Monolayer Formed at Room Temperature on Ionic Model Substrates. *Phys. Rev. Lett.* **2009**, *103*, 137801.

(16) Rezus, Y. L. A.; Bakker, H. J. Observation of Immobilized Water Molecules around Hydrophobic Groups. *Phys. Rev. Lett.* **2007**, *99*, 148301.

(17) Laage, D.; Stirnemann, G.; Hynes, J. T. Why Water Reorientation Slows without Iceberg Formation around Hydrophobic Solutes. *J. Phys. Chem. B* **2009**, *113*, 2428−2435.
(18) Pham, V. T.; Penfold, T. J.; van der Veen, R. M.; Lima, F.; El Nahhas, A.; Johnson, S. L.; Beaud, P.; Abela, R.; Bressler, C.; Tavernelli, I.; Milne, C. J.; Chergui, M. Probing the Transition from Hydrophilic to Hydrophobic Solvation with Atomic Scale Resolution. *J. Am. Chem. Soc.* **2011**, *133*, 12740−12748.
(19) Plimpton, S. Fast Parallel Algorithms for Short-Range Molecular-Dynamics. *J. Comput. Phys.* **1995**, *117*, 1−19.
(20) Berendsen, H. J. C.; Grigera, J. R.; Straatsma, T. P. The Missing Term in Effective Pair Potentials. *J. Phys. Chem.* **1987**, *91*, 6269−6271.
(21) Reif, M. M.; Hunenberger, P. H. Computation of Methodology-Independent Single-Ion Solvation Properties from Molecular Simulations. IV. Optimized Lennard-Jones Interaction Parameter Sets for the Alkali and Halide Ions in Water. *J. Chem. Phys.* **2011**, *134*, 144103.
(22) Irudayam, S. J.; Henchman, R. H. Solvation Theory to Provide a Molecular Interpretation of the Hydrophobic Entropy Loss of Noble-Gas Hydration. *J Phys.: Condens. Matter* **2010**, *22*.
(23) Ashbaugh, H. S.; Collett, N. J.; Hatch, H. W.; Staton, J. A. Assessing the Thermodynamic Signatures of Hydrophobic Hydration for Several Common Water Models. *J. Chem. Phys.* **2010**, *132*, 124504−124507.
(24) Hirschfelder, J. O.; Curtiss, C. F.; Bird, R. B. *Molecular Theory of Gases and Liquids*;Wiley: New York, 1954.
(25) Lin, S. T.; Blanco, M.; Goddard, W. A. The Two-Phase Model for Calculating Thermodynamic Properties of Liquids from Molecular Dynamics: Validation for the Phase Diagram of Lennard-Jones Fluids. *J. Chem. Phys.* **2003**, *119*, 11792−11805.
(26) Lin, S. T.; Maiti, P. K.; Goddard, W. A. Two-Phase Thermodynamic Model for Efficient and Accurate Absolute Entropy of Water from Molecular Dynamics Simulations. *J. Phys. Chem. B* **2010**, *114*, 8191−8198.
(27) Zhang, C.; Spanu, L.; Galli, G. Entropy of Liquid Water from Ab Initio Molecular Dynamics. *J. Phys. Chem. B* **2011**, *115*, 14190−14195.
(28) Pascal, T. A.; Goddard, W. A.; Jung, Y. Entropy and the Driving Force for the Filling of Carbon Nanotubes with Water. *Proc. Natl. Acad. Sci. U.S.A.* **2011**, *108*, 11794−11798.
(29) Pascal, T. A.; He, Y.; Jiang, S.; Goddard, W. A. Thermodynamics of Water Stabilization of Carboxybetaine Hydrogels from Molecular Dynamics Simulations. *J. Phys. Chem. Lett.* **2011**, *2*, 1757−1760.
(30) Spanu, L.; Donadio, D.; Hohl, D.; Schwegler, E.; Galli, G. Stability of Hydrocarbons at Deep Earth Pressures and Temperatures. *Proc. Natl. Acad. Sci. U.S.A.* **2011**, *108*, 6843−6846.
(31) Abraham, M. H. Free Energies, Enthalpies, and Entropies of Solution of Gaseous Nonpolar Nonelectrolytes in Water and Nonaqueous Solvents. The Hydrophobic Effect. *J. Am. Chem. Soc.* **1982**, *104*, 2085−2094.
(32) Hummer, G.; Pratt, L. R.; Garcia, A. E. Free Energy of Ionic Hydration. *J. Phys. Chem.* **1996**, *100*, 1206−1215.
(33) Straatsma, T. P.; Berendsen, H. J. C. Free-Energy of Ionic Hydration. Analysis of a Thermodynamic Integration Technique to Evaluate Free-Energy Differences by Molecular-Dynamics Simulations. *J. Chem. Phys.* **1988**, *89*, 5876−5886.
(34) DeMille, R. C.; Molinero, V. Coarse-Grained Ions without Charges: Reproducing the Solvation Structure of Nacl in Water Using Short-Ranged Potentials. *J. Chem. Phys.* **2009**, *131*, 034107.
(35) Omta, A. W.; Kropman, M. F.; Woutersen, S.; Bakker, H. J. Negligible Effect of Ions on the Hydrogen-Bond Structure in Liquid Water. *Science* **2003**, *301*, 347−349.
(36) Geissler, P. L.; Smith, J. D.; Saykally, R. J. The Effects of Dissolved Halide Anions on Hydrogen Bonding in Liquid Water. *J. Am. Chem. Soc.* **2007**, *129*, 13847−13856.
(37) Huang, D. M.; Geissler, P. L.; Chandler, D. Scaling of Hydrophobic Solvation Free Energies. *J. Phys. Chem. B* **2001**, *105*, 6704−6709.
(38) Ashbaugh, H. S.; Pratt, L. R. Colloquium: Scaled Particle Theory and the Length Scales of Hydrophobicity. *Rev. Mod. Phys.* **2006**, *78*, 159−178.
(39) Bryantsev, V. S.; Diallo, M. S.; Goddard, W. A. Computational Study of Copper(II) Complexation and Hydrolysis in Aqueous Solutions Using Mixed Cluster/Continuum Models. *J. Phys. Chem. A* **2009**, *113*, 9559−9567.
(40) van der Spoel, D.; Caleman, C.; Hub, J. S.; van Maaren, P. J. Atomistic Simulation of Ion Solvation in Water Explains Surface Preference of Halides. *Proc. Natl. Acad. Sci. U.S.A.* **2011**, *108*, 6838−6842.